

Formation of a Non-Thickness-Limited Titanium Dioxide Mesosponge and its Use in Dye-Sensitized Solar Cells**

Doohun Kim, Kiyoun Lee, Poulomi Roy, Balaji I. Birajdar, Erdmann Spiecker, and Patrik Schmuki*

In 1998, Melody et al. introduced an electrochemical anodization process that was reported to lead to so-called non-thickness-limited (NTL) oxide growth for some refractory metals (in particular Ta).^[1] By anodization of Ta at 150–180 °C in glycerol/K₂HPO₄ solutions, oxide layers several tens of micrometers thick could be grown without observing a drop in the growth rate with time. In further work, this process was used with Ti, but was not successful.^[2] Herein, we show that by anodizing Ti under adequate conditions, a non-thickness-limited oxide can indeed be grown. Moreover, by a subsequent selective etching treatment of these layers, a connected, ordered, and mesoporous TiO₂ network can be obtained and is suitable for application in high-efficiency dye-sensitized solar cells.

Over the past 30 years, TiO₂ has attracted wide interest from both the scientific and the technological communities because of its high number of potential applications. In particular, its unique electronic properties make the material attractive, for example for photocatalysis,^[3] as well as for solar energy conversion.^[4–8] For this type of application, a large specific surface area is required, and therefore efficient photovoltaic or catalytic electrodes are commonly based on sintered or compacted anatase nanoparticles. In Grätzel-type solar cells, particle sizes are typically around 10 nm, which are assembled to approximately 10 µm thick porous layers by doctor-blading or spin-coating approaches.^[6–8] The layers then are sensitized with a suitable dye^[9] and mounted into various solar cell configurations.^[5,10,11,16]

Another versatile technique for the production of defined oxide layers is anodization of a suitable metal substrate. However, in the case of Ti, anodic layers of TiO₂ are formed under most conditions with a compact morphology that is typically limited to a thickness of some 100 nm. To date, only the anodic growth of TiO₂ nanotube layers seemed promising

for the production of nanostructured geometries that have thicknesses in the 10 µm range and are interesting for solar cell applications.^[10–19] Herein, we introduce an anodization and selective etching approach to form a robust and ordered mesoporous TiO₂ network (TiO₂ mesosponge) that is tens of micrometers thick and is formed directly on a Ti substrate.

Figure 1 shows a SEM cross section of a 15–18 µm thick layer of TiO₂ grown by anodization of a Ti sheet in 10 wt % K₂HPO₄ in glycerol at (180 ± 1) °C. It was crucial to carefully optimize the experimental conditions in order to achieve the growth of such layers. In particular, the temperature, pre-anodization time, and anodization current have to be accurately controlled (details are given in the Supporting Information). Under the optimized conditions and after extended anodization, such layers can be grown to thicknesses greater than 50 µm. If the conditions are not sufficiently maintained, only compact or nanoporous oxide layers of some 100 nm thickness could be observed. Thick layers, as shown in Figure 1, have a comparably tight oxide morphology with some nanoscopic channels that are apparent in SEM (scanning electron microscopy; Figure 1b) and TEM (Figure 1c,d) images. The SEM image in Figure 1b shows that the channels typically have a preferred orientation perpendicular to the surface. This orientation is further confirmed by the TEM image (Figure 1c) and the HRTEM image (Figure 1d), which were taken in plan-view geometry and show most of the channels in an edge-on orientation. The width of these pores is in the range 5–10 nm. A main drawback in terms of applications is that the spacing between the nanoscopic channels is wide (ca. 20–50 nm), as apparent from the SEM inset in Figure 1b. However, if this structure is adequately chemically etched, a highly regular and defined sponge structure as shown in the SEM image of Figure 1e,f is obtained. This structure was etched for 1 h in 30 wt % H₂O₂ under ultrasonication. A very regular mesoporous morphology is obtained over the entire sample thickness (Figure 1e), with typical TiO₂ sizes in the range 5–10 nm and pores of approximately 10 nm (Figure 1f). In comparison with the “as-formed” layer, a much more open structure is present.

Figure 2a shows the XRD pattern of the layers of Figure 1. The results reveal that the “as-formed” porous layers before and after etching are amorphous but contain some anatase and rutile crystallites. The diffractogram shown as inset in Figure 1d confirms the mostly amorphous nature but furthermore indicates that some metallic Ti may still be present in the structure. To make use of TiO₂ in applications based on photoexcitation, a crystalline structure is desired to eliminate defects associated with the amorphous material.^[20,21] To crystallize the mesoporous TiO₂ layers, we

[*] D. Kim, K. Lee, Dr. P. Roy, Dr. P. Schmuki
Department of Materials Science and Engineering, WW4-LKO
University of Erlangen-Nuremberg
Martensstrasse 7, 91058 Erlangen (Germany)
Fax: (+49) 9131-852-7582
E-mail: schmuki@ww.uni-erlangen.de
Homepage: <http://www.lko.uni-erlangen.de/>

Dr. B. I. Birajdar, Dr. E. Spiecker
Department of Materials Science and Engineering, WW7
University of Erlangen-Nuremberg
Cauerstrasse 6, 91058 Erlangen (Germany)

[**] We acknowledge DFG and the DFG Cluster of Excellence (EAM) for financial support.

Supporting information for this article is available on the WWW under <http://dx.doi.org/10.1002/anie.200904455>.

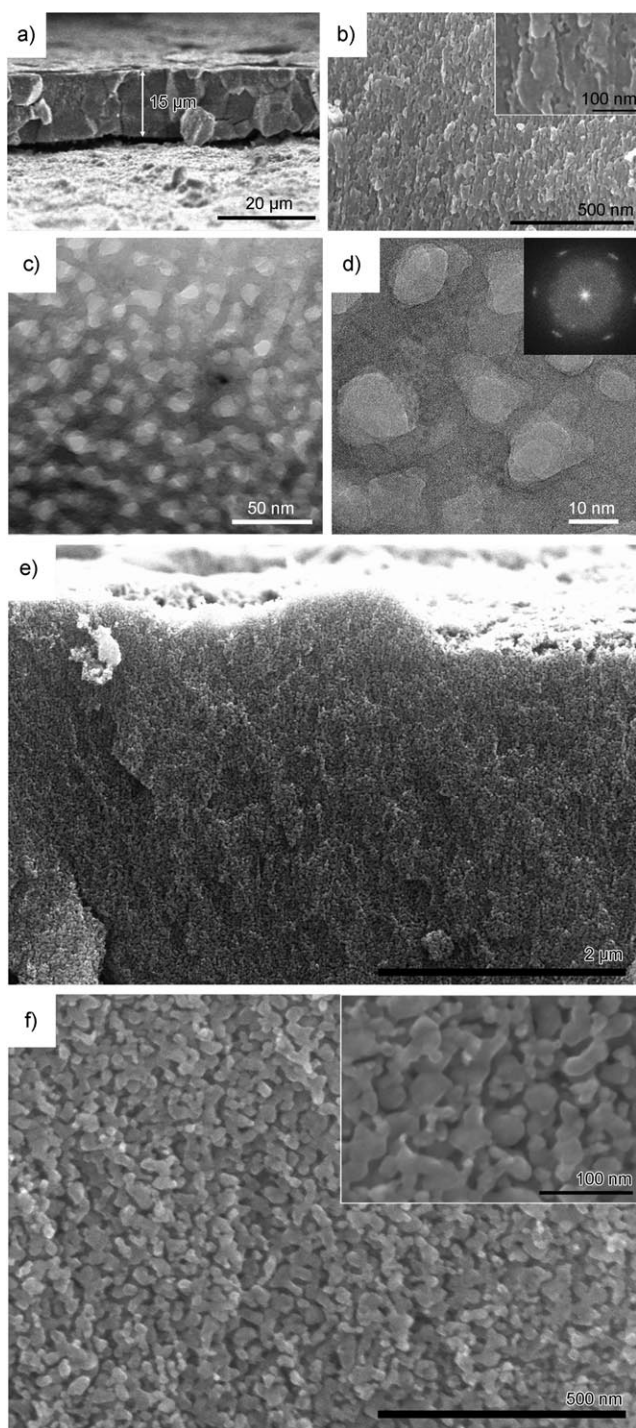


Figure 1. Steps in TiO_2 mesosponge formation. a, b) SEM images of a non-thickness-limited TiO_2 layer formed on Ti by anodization in 10 wt% K_2HPO_4 in glycerol at $(180 \pm 1)^\circ\text{C}$. c, d) TEM image and HRTEM image of the TiO_2 layer. The inset shows the corresponding diffractogram. e, f) SEM images after etching in 30 wt% H_2O_2 for 1 h, leading to a highly regular sponge morphology.

annealed them in air at 450°C . The TEM results in Figure 2d,e show that after annealing, the open structure seen in Figure 1 f is maintained and that the material is fully crystalline. From the XRD results in Figure 2c, it is evident that a mixed anatase/rutile crystal structure was formed. The

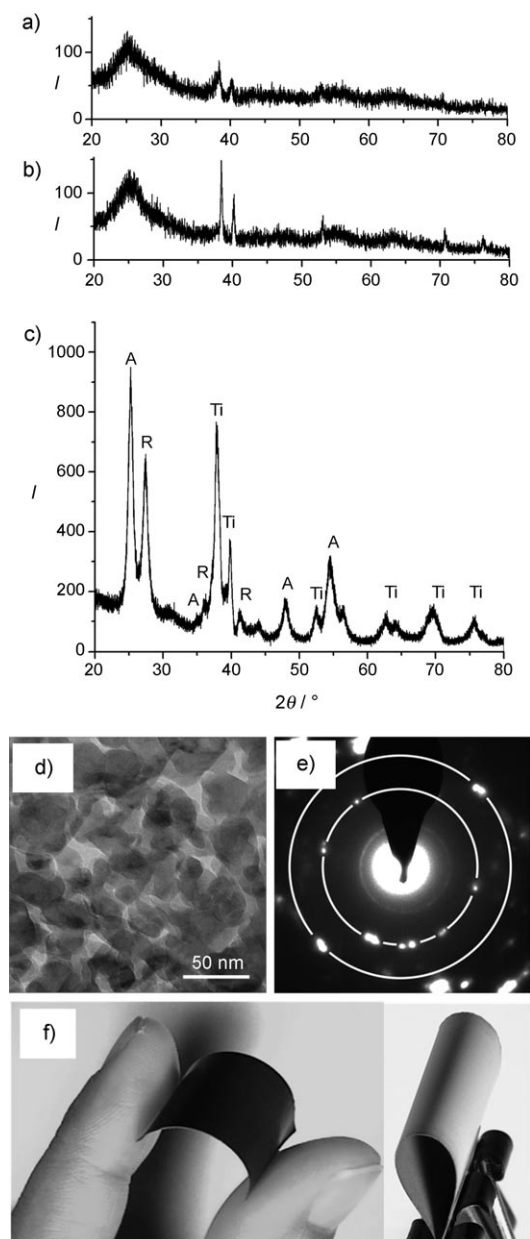


Figure 2. Structural characterization of the TiO_2 mesoporous layer after different fabrication and annealing steps. XRD of layers a) after anodic formation, b) after etching, and c) after thermal treatment at 450°C . The peaks are annotated as anatase (A), rutile (R), Ti metal (Ti). d, e) TEM image and SAED pattern for the material after annealing. f) Flexibility and stability of the layer after annealing.

selected area diffraction (SAED) pattern in Figure 2 confirms crystallization and formation of anatase. XPS results (see Figure S1 in the Supporting Information) show that the “as formed” NTL oxide layer consist of TiO_2 that contains a comparably small amount of potassium and phosphorous (1.33 atom % and 0.69 atom %, respectively). After etching and annealing, the contaminants are removed from the layer. As expected, the surface hydroxide content is strongly reduced after annealing (as apparent from the XPS O1s signal; see Figure S1 in the Supporting Information), and the peak shape and position are in good agreement with anatase

TiO₂.^[21,22] Figure 2 f shows how well the layers adhere to the surface, that is, not only do the layers remain intact after intense bending (allowing for example flexible solar cells) but also other intense mechanical treatment (such as scratching) does not lead to flaking (lift off) of the TiO₂ mesosponge layer (this observation is in contrast, for example, to TiO₂ nanotube layers).

In order to demonstrate the feasibility of using TiO₂ mesosponge layers in Grätzel-type DSSCs, we assembled cells (Figure 3 a) and characterized their performance using

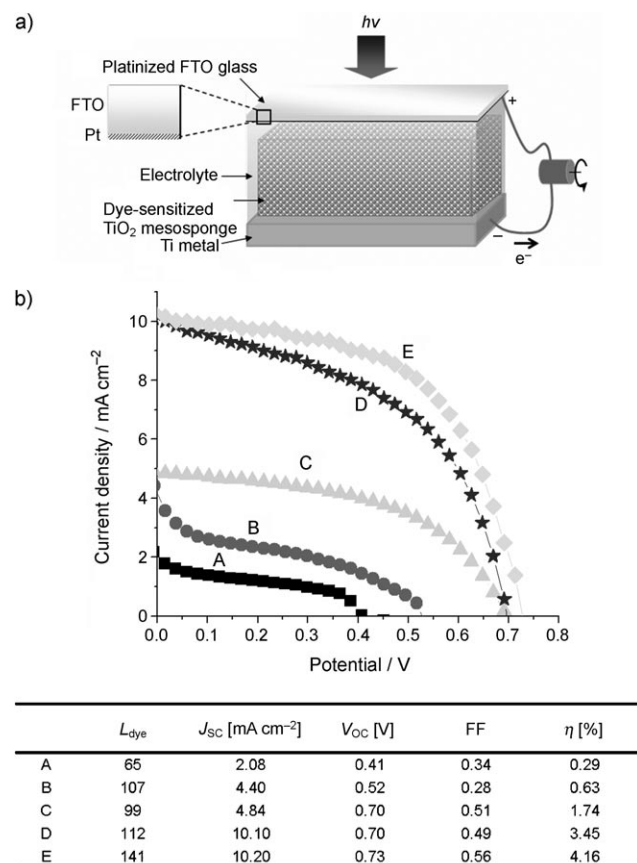


Figure 3. a) Schematic representation of solar cell construction using TiO₂ mesosponge layers grown on Ti substrates. b) *I*-*V* curves obtained from solar cells for different stages of sponge formation and for differently etched sponge layers. The table gives extracted photo-voltaic characteristics and dye loading of the dye-sensitized TiO₂ layers. A) Non-etched and non-annealed, B) etched in H₂O₂ and non-annealed, C) non-etched and annealed, D) etched in H₂O₂ and annealed, E) etched in oxalic acid and annealed. L_{dye} = dye loading, J_{sc} = short-circuit current, V_{oc} = open-circuit voltage, FF = fill factor, η = efficiency.

an AM 1.5 solar simulator setup (see the Supporting Information). From the *I*-*V* curves shown in Figure 3 b, it is evident that for the “as formed” nanoporous network, only efficiencies less than 1 % could be obtained, even after extended dye sensitization and electrolyte penetration times. If the “as-formed” material is crystallized by annealing, the efficiency (η) can be increased, however the comparably low values ($\eta \approx 1$ –1.5 %) indicate that in the as-anodized and annealed

state, the pore structure is not sufficiently open to allow an efficient penetration of the dye and/or iodine electrolyte. Only after pore widening and annealing can efficient dye sensitization be carried out and solar cell structures with an efficiency greater than 4 % can be easily obtained. The increase in available surface area after the etching process is evident from dye desorption measurements that yield a dye loading that is more than twice as high for the etched material. In fact, the specific dye loading of the TiO₂ mesosponge is 2–3 times higher than for TiO₂ nanotubes, which are currently intensively investigated.^[17,19]

Moreover, an efficiency of 4.2 % was achieved in our first attempts (under nonoptimized conditions). This value is higher than the best efficiency for solar cells based on pure TiO₂ nanotubes ($\eta \approx 3.3$ %^[11,14,19] without using additional TiO₂ nanoparticle decoration^[19,23]). In fact, the mesosponge morphology shown in Figure 1 e, f very much resembles the feature size and arrangement of the nanoparticulate layers currently used in commercial Grätzel-type DSSCs.^[3]

The strong interlinkage of the TiO₂ framework is a clear advantage of the anodic mesoporous TiO₂ structure. The feature size and distribution in the sponge depends significantly on the electrochemical treatment and on the used etchant (see Figures S2 and S3 in the Supporting Information). Photomodulation measurements (intensity modulated photocurrent and photovoltage spectroscopy; see Figure S2 in the Supporting Information) indicate the strong influence of the sponge morphology on carrier transport and recombination times. These findings strongly suggest that the mesosponge structure can still be significantly improved by optimizing both the formation and the etching procedure.

We have shown how a highly regular and robust mesoporous TiO₂ structures with thicknesses greater than 50 μm can be directly formed on Ti by using a simple anodization process followed by a selective chemical etching step. The partially amorphous material needs to be fully crystallized to an anatase or rutile crystal structure for many functional applications. We have shown how effectively the material can be used in Grätzel-type DSSCs, and we have shown efficiencies better than the best pure TiO₂ nanotube solar cells in our first attempts. This achievement is even more remarkable as the results reported here are far from being optimized. However, it can be expected that the material finds even wider significance in all fields of TiO₂ applications where a considerably thicker and mesoporous network is required (for example, in photocatalysis, biomedicine, or water splitting approaches).

Received: August 9, 2009

Published online: November 4, 2009

Keywords: dyes/pigments · mesoporous materials · solar cells · titanates · titanium

- [1] B. Melody, T. Kinard, P. Lessner, *Electrochem. Solid-State Lett.* **1998**, *1*, 126.
- [2] H. Habazaki, Y. Oikawa, K. Fushimi, K. Shimizu, S. Nagata, P. Skeldon, G. E. Thompson, *Electrochim. Acta* **2007**, *53*, 1775.
- [3] A. Fujisima, K. Honda, *Nature* **1972**, *238*, 37.

- [4] B. O'Regan, M. Grätzel, *Nature* **1991**, 353, 737.
- [5] M. Grätzel, *Nature* **2001**, 414, 338.
- [6] M. Grätzel, *J. Photochem. Photobiol. C* **2003**, 4, 145.
- [7] M. Grätzel, *J. Photochem. Photobiol. A* **2004**, 164, 3.
- [8] L. Schmidt-Mende, M. Grätzel, *Thin Solid Films* **2006**, 500, 296.
- [9] A. Mishra, M. K. R. Fischer, P. Bauerle, *Angew. Chem.* **2009**, 121, 2510; *Angew. Chem. Int. Ed.* **2009**, 48, 2474.
- [10] A. Ghicov, S. Albu, R. Hahn, D. Kim, T. Stergiopoulos, J. Kunze, C. A. Schiller, P. Falaras, P. Schmuki, *Chem. Asian J.* **2009**, 4, 520.
- [11] P. Roy, D. Kim, K. Lee, E. Spiecker, P. Schmuki, *Nanoscale*, in press.
- [12] J. M. Macak, H. Tsuchiya, A. Ghicov, P. Schmuki, *Electrochem. Commun.* **2005**, 7, 1133.
- [13] K. Zhu, T. B. Vinzant, N. R. Neale, A. J. Frank, *Nano Lett.* **2007**, 7, 3739.
- [14] K. Zhu, N. R. Neale, A. Miedaner, A. J. Frank, *Nano Lett.* **2007**, 7, 69.
- [15] R. Hahn, T. Stergiopoulos, J. M. Macak, D. Tsoukleris, A. G. Kontos, S. P. Albu, D. Kim, A. Ghicov, J. Kunze, P. Falaras, P. Schmuki, *Phys. Status Solidi* **2007**, RRL 1, R135.
- [16] J. R. Jennings, A. Ghicov, L. M. Peter, P. Schmuki, A. B. Walker, *J. Am. Chem. Soc.* **2008**, 130, 13364.
- [17] D. Kim, A. Ghicov, S. P. Albu, P. Schmuki, *J. Am. Chem. Soc.* **2008**, 130, 16454.
- [18] D. Kim, A. Ghicov, P. Schmuki, *Electrochem. Commun.* **2008**, 10, 1835.
- [19] P. Roy, D. Kim, I. Paramasivam, P. Schmuki, *Electrochem. Commun.* **2009**, 11, 1001.
- [20] A. Fujishima, X. Zhang, D. A. Tryk, *Surf. Sci. Rep.* **2008**, 63, 515.
- [21] U. Diebold, *Surf. Sci. Rep.* **2003**, 48, 53.
- [22] J. E. Moulder, W. F. Stickle, P. E. Sobol, K. D. Bomben in *Handbook of X-ray Photoelectron Spectroscopy* (Ed.: J. Chastain), Perkin-Elmer Corporation, Minnesota, **1992**.
- [23] J. H. Park, T.-W. Lee, M. G. Kang, *Chem. Commun.* **2008**, 2867.